

Microcrimped Collagen Fiber-Elastin Composites

By Jeffrey M. Caves, Vivek A. Kumar, Wenjun Xu, Nisarga Naik, Mark G. Allen, and Elliot L. Chaikof*

Emerging biomaterials based upon analogues of native extracellular matrix proteins provide an opportunity to create protein scaffolds that mimic tissue mechanical behavior and guide cellular responses. However, in order to reproduce macroscale tissue properties, protein analogues must be endowed with appropriate microstructural features. In particular, the crimped or wavy microstructure of native collagen fibers, with a periodicity of 10–200 μm , contributes in a significant manner to the compliance, strength, and durability of soft tissues. In this report, we describe a templating strategy based upon the application of micropatterned elastomeric substrates, which yields dense, aligned arrays of synthetic collagen microfibers that display a well-defined microcrimped pattern. Following crosslinking with glutaraldehyde vapor, fiber arrays were embedded in a recombinant elastin protein polymer,^[1] which contributes to the resilience of the composite structure by bearing tensile loads at low strains, analogous to a native elastin fiber network.^[2,3] We demonstrate the preservation of fiber crimp after repetitive cyclic loading, as well as the assembly of hierarchical microcrimped multilamellar composites with mechanical responses similar to native tissues.

The periodic waviness of fibrous collagen is observed in nearly all human tissues, including blood vessels, valve leaflets, intestine, tendon, and intervertebral discs.^[4–6] The morphological features of crimp structure has been characterized as planar zig-zag,^[7] sinusoid,^[8] or helical^[9,10] with wavelengths between 10 to 200 μm . Crimp ensures that at low levels of tensile strain, loads are sustained both by the surrounding matrix and the fiber network. Typically, fibers straighten as a load is imposed with an observed transition from low to high tissue stiffness.^[4,5,11,12] These mechanisms serve to enhance compliance at low strain while generating greater strength as load increases. Since physiologic strains are imposed at levels of stress where fibers are often not fully extended, the propensity for fatigue-related fiber damage is minimized. All told, fiber crimp has evolved as an important bioengineering principle that affords a favorable combination of compliance, strength, and durability.

A set of techniques using soft, contracting substrates to shape thin coatings of high modulus materials into crimped, wrinkled,

and wavy structures has recently emerged.^[13–19] For example, Bowden and colleagues deposited metal films on heated PDMS and noted that, upon cooling, the contraction of the PDMS buckled the metal layer into sophisticated patterns of wrinkles.^[13] However, in these cases the extent of waviness is limited by the extent of inducible thermal shrinkage. Alternatively, an elastomeric substrate may be mechanically stretched prior to the application of a thin film,^[15] array of nanoribbons,^[14,16] integrated circuit,^[17] or carbon nanotubes,^[18] with relaxation of stretch producing defined wavy structures. Collectively, these studies have led to the fabrication of controlled micro- and nanoscale waveforms. However, microcrimping techniques have not been developed that are suitable for biological materials, such as collagen fibers.

Controlled deformation of a flexible microridged membrane dictates microcrimp fiber morphology. Flexible polyurethane microridges with a buttress-rectangular profile were fabricated following photolithographic and micromolding techniques. Collagen fibers are sandwiched between a smooth base substrate and a microridged membrane, both pre-extended to a desired strain, strain relaxed to induce microcrimp features, and fibers crosslinked by glutaraldehyde vapor (Fig. 1a–d). Scanning electron microscopy revealed a repetitive crimp pattern, resembling native collagen with the degree of crimp directly related to the magnitude of imposed pre-extension strain (Fig. 1h–k).

Fiber embedding within an elastin-mimetic protein matrix and subsequent lamination of multiple, individual, fiber-reinforced sheets was accomplished by a thermally controlled sol-gel process. As detailed elsewhere, an aqueous solution of elastin-mimetic triblock protein polymer forms a physically crosslinked gel above 13 °C.^[20] Single sheets of embedded microcrimped fibers were fabricated by dispensing a cooled solution of protein over an array of crimped fiber. An acrylic plate was then applied, the assembly warmed, and a fiber-reinforced elastin composite separated from the mold (Fig. 1e and f).

Three-dimensional analysis of embedded fibers confirmed preservation of crimp structure within the protein matrix (Fig. 2a–c). Exposure to glutaraldehyde vapor was used to preserve the crimp structure before the fibers were hydrated with the elastin-mimetic protein and embedded within the sheet. Crimp of $3.1\% \pm 0.4\%$ and $9.4\% \pm 2.9\%$ was observed for fibers templated at pre-extension strains of 15% and 30%, respectively. Observed differences between pre-extension and degree of crimp presumably reflect fiber shortening induced by drying steps and matrix swelling after fiber embedding. Indeed, peak-to-peak periodicity was $(143 \pm 5) \mu\text{m}$ for fibers embedded in a hydrated protein matrix, but decreased to $(127 \pm 5) \mu\text{m}$ for dry fibers in a non-embedded state.

[*] Prof. E. L. Chaikof, Dr. J. M. Caves, V. A. Kumar
Departments of Biomedical Engineering and Surgery
Emory University/Georgia Institute of Technology
101 Woodruff Circle, Rm 5105, Atlanta, GA 30322 (USA)
E-mail: echaiko@emory.edu

W. Xu, N. Naik, Prof. M. G. Allen
Schools of Electrical and Computer Engineering, Georgia Institute of
Technology
791 Atlantic Dr., MiRC 120, Atlanta, GA 30332 (USA)

DOI: 10.1002/adma.200903612

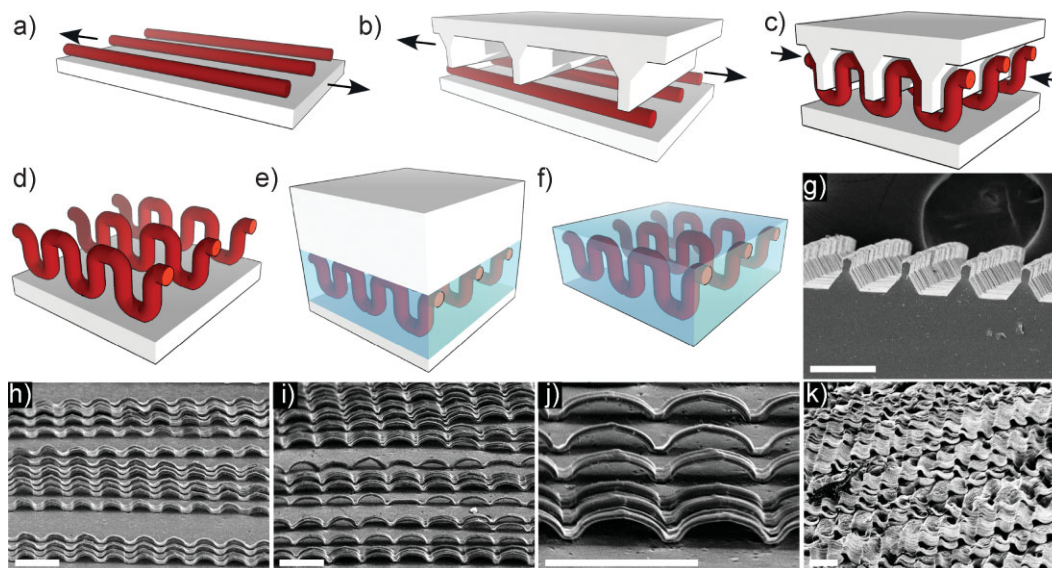


Figure 1. Microcrimping method and scanning electron microscopy of crimped collagen microfibers. A parallel array of hydrated synthetic collagen fibers is placed on a pre-extended polyurethane substrate (a). The polyurethane buttressed-rectangular membrane is pre-extended and clamped over collagen fiber (b). The pre-extension in the substrate and buttressed rectangular membrane is relaxed to generate microcrimp, and the assembly is frozen at $-80\text{ }^{\circ}\text{C}$ (c). The buttressed-rectangular membrane is removed and the frozen fiber array is transferred to room temperature glutaraldehyde vapor for 24 h (d). A cooled solution of elastin-mimetic protein is distributed over the microcrimped fiber and pressed into a thin layer with a flat sheet of acrylic (e). After warming to gel the elastin-mimetic protein, the fiber-reinforced layer is separated from the acrylic and polyurethane surfaces (f). SEM of the polyurethane buttressed-rectangular membrane (g), and synthetic collagen fiber arrays templated with 30 and 40% pre-extension after drying and removal of the microridged membrane (h,i). High magnification image of fibers crimped with 40% pre-extension is shown in (j), and a dense sheet of microcrimped fiber in (k). Scale bars $200\text{ }\mu\text{m}$.

A fiber-reinforced multilamellar composite was generated by stacking single sheets. Stacks were briefly cooled below the transition temperature of the elastin-mimetic protein matrix and subsequently re-warmed. This process dissolved and then re-gelled the elastin-mimetic protein matrix, bonding the individual sheets into a cohesive, multilamellar structure (Fig. 2d and e). Although all fibers are parallel to one another within a single sheet, by varying the orientation of successive layers multi-angle fiber composites can be generated.

Microcrimping enhances low-strain compliance of fiber-reinforced composites. Composites display a transition between low and high modulus regimes at a tensile strain dictated by the degree of fiber crimp (Fig. 3a, Table S1). This ‘strain-at-transition’ was $1.9\% \pm 0.6\%$ for single sheets with straight fibers, but increased significantly to $4.6\% \pm 0.9\%$ and $13.3\% \pm 0.7\%$ for composites comprised of crimped fibers templated at pre-extension strains of 15% and 30%, respectively ($p < 0.05$), which also closely reflected measured degrees of crimp (0%; 3.1%; 9.4%). In the pre-transition region, the Young’s modulus of microcrimped specimens ranged from 1 to 5 MPa, approximating soft tissues such as the artery wall (0.1 to 2.0 MPa).^[21] Strain-at-failure doubled when composites were fabricated from crimped fibers templated at a pre-extension strain of 30% ($p < 0.01$). Of note, microcrimp morphology was retained following 50 000 loading cycles at 1 Hz (Fig. S1).

The fabrication of composites in which fiber arrays are organized in a distinct in-plane orientation provided an additional approach to tune both compliance and strain-at-failure. Young’s modulus was reduced and strain-at-transition increased when multilamellar structures were fabricated from fibers orientated at

cross-angles of $\pm 25^{\circ}$, in the presence or absence of crimp ($p < 0.05$, Fig. 3c, Table S1). This behavior is anticipated since fibers do not bear load directly, but rotate into alignment as the composite is stretched. However, when angled-fiber structures were composed of crimped fibers, a further increase in strain-at-failure was observed ($p < 0.05$). Overall, tensile strengths of all configurations met or exceeded those of many native tissues, including human urinary bladder ((0.270 ± 0.140) MPa),^[22] pulmonary artery ((0.385 ± 0.045) MPa),^[23] and aorta ((1.72 ± 0.89) MPa, mean \pm SD).^[24] Significantly, both fiber angle and microcrimp morphology provide complimentary design variables that can be independently adjusted to tailor the properties of soft tissue equivalents. For example, composites of straight fibers oriented at $\pm 25^{\circ}$ and those of microcrimped fibers in parallel orientation both produced mechanical responses that closely matched bovine pericardium. This animal derived tissue is currently used to fabricate bioprosthetic heart valves, vascular patches, and blood vessel substitutes (Fig. 3d).^[25]

The design of synthetic tissue composites comprised of crimped collagen fiber arrays, organized at defined cross-fiber orientations, will provide an important mechanism to tailor tissue compliance, reduce imposed tissue stresses, and improve tissue durability. Presumably, this effect will be greatest under conditions in which the engineered tissue is subjected to repetitive tensile or compressive loading forces, as is the case for a variety of cardiovascular and musculoskeletal structures.^[26,27] Crimped fiber composites will also facilitate the fabrication of engineered tissues whose biomechanical microenvironment is optimized for desirable cellular responses.^[27–29] Moreover, we speculate that microcrimped fibers may contribute to the control

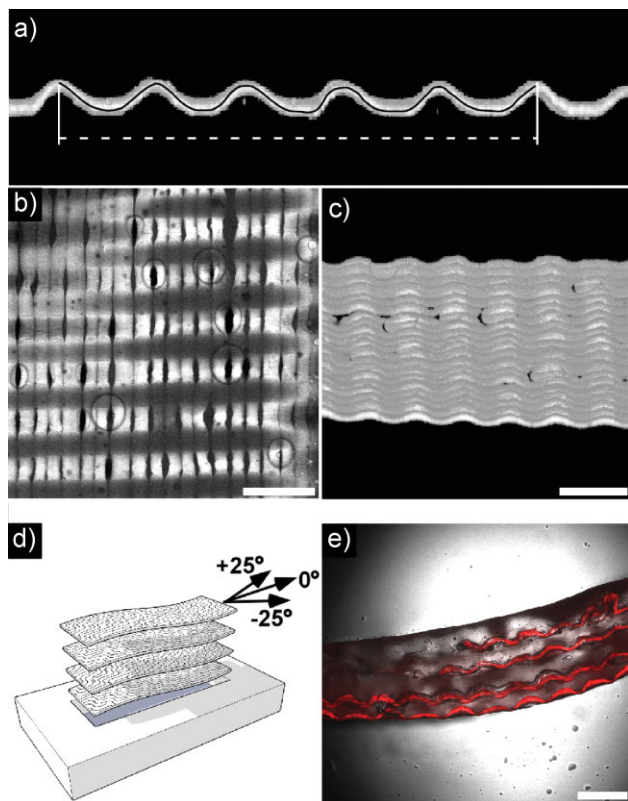


Figure 2. Embedding of microcrimped collagen microfibers within an elastin matrix and fabrication of multilamellar collagen fiber-reinforced elastin sheets. Confocal laser scanning microscopy is used to selectively image the hydrated collagen fibers within a single elastin lamella. The degree of crimp is calculated from the center-line (solid black) and straight-line (dashed white) lengths (a). Fibers in a single lamella sheet pass in and out of the confocal plane due to crimp (b). A 3D reconstruction of the collagen fiber array in (b) demonstrates crimped fiber structure in a single lamellar sheet (c). Multilamellar sheets are fabricated by stacking single sheets, cooling to disrupt physical crosslinks of the protein polymer matrix, and then warming to restore crosslinking and facilitate interlayer bonding. Fibers are oriented parallel to the long axis of the laminate (0°) or alternate at $\pm 25^\circ$ to the long axis (d). Microcrimping was observed by CLSM in multilamellar sheets (e). Scale bars $200\ \mu\text{m}$.

of cellular organization of constructs, either pre-seeded with cells or otherwise designed to induce cellular in-growth after implantation. To achieve cell-populated structures, the presented technique can be modified to replace glutaraldehyde with more cytocompatible crosslinkers, such as hexamethylene diisocyanate or genipin.

In summary, oriented arrays of synthetic collagen fibers have been fabricated with microcrimped structure approaching the scale of naturally occurring collagen crimp. After embedding fibers in an elastin-like matrix, crimp morphology is largely retained with substantial preservation of form under repetitive cyclic loading. Cohesive, multilamellar sheets with defined fiber orientations were generated with enhanced strain-at-failure and a transition between low and high modulus regions at strains dictated by the degree of crimp. Adjustment of fiber orientation provides an additional means to tailor mechanical responses. Collectively, microcrimped composites represent an important

step towards the development of extracellular matrix analogs that mimic native tissues.

Experimental

Production of synthetic collagen fiber, recombinant elastin-mimetic triblock protein polymer, and flexible microridged membranes: Synthetic collagen fibers were produced using a lab scale fiber spinning system, as previously reported [30]. Genetic engineering, expression, purification, and characterization of the elastin-mimetic protein polymer, designated **LysB10**, has been described elsewhere [1]. The buttress-rectangular microridged membrane was molded from polydimethylsiloxane (PDMS) master molds. Additional details can be found in the Supporting Information.

Method for scalable microcrimping of synthetic collagen fibers: Before microcrimping, fibers were arranged as dense parallel sheets by winding about rectangular frames. The microcrimping system consisted of a lead screw assembly, an ultrasoft smooth viscoelastic base membrane, and the microridged membrane. The base membrane was fastened to the lead screw assembly and a pre-extension tensile strain of 15 to 55% was applied. An array of collagen fibers were fastened to the extended base membrane, hydrated with ddH₂O for 15 min, excess water removed, and the microridged membrane applied at the same tensile strain as the pre-extended base membrane. Adjustment to the lead screw assembly relaxed the pre-extension in both membranes and microcrimped the fiber array. The system was cooled to -80°C for 2 h, warmed to -20°C for 4 h, followed by removal of the microridged membrane. Fibers on the base membrane were transferred to a desiccator saturated with vapor from a 25% glutaraldehyde solution and stored at room temperature for 24 h.

Formation of elastin-like protein polymer single and multilamellar structures with integrated microcrimped collagen fibers: A 10 wt % solution of elastin protein polymer was deposited onto a crimped fiber array, initially frozen at -80°C . An acrylic sheet was applied to evenly spread the solution between shims, which gelled within 25 min at room temperature. Specimens were then crosslinked in a 0.5% glutaraldehyde solution for 24 h at 37°C , which yielded a single $80\ \mu\text{m}$ -thick sheet. To create a multilamellar composite, non-crosslinked, sheets with fibers oriented either parallel or at $\pm 25^\circ$ were stacked, cooled to 4°C for 12 h, and then heated to 37°C for 30 min. Samples were then crosslinked in 0.5% glutaraldehyde.

Microscopic analysis and degree of crimp: Scanning electron microscopy was used to image dry fibers. Hydrated, embedded fibers were imaged with confocal laser scanning microscopy (CLSM). The degree of fiber crimp, C , was measured from 3D reconstructions of microcrimped fiber. Degree of crimp was defined as:

$$C = (l_c - l_s) / l_s \times 100\% \quad (1)$$

where l_c and l_s are the center-line and the straight-line distances, respectively.

Mechanical analysis: Tensile testing was performed on a dynamic mechanical thermal analyzer (DMTA V, Rheometric Scientific, Inc., Newcastle, DE). Cyclic loading was performed on an Electroforce 3200 test instrument (Bose Co., Eden Prairie, MN). In both cases, samples were immersed in PBS at 37°C throughout the mechanical tests.

Acknowledgements

Supported by NIH R01HL083867, R01HL60464, and R01HL71336. JMC was a recipient of a NSF Graduate Fellowship Award. Supporting Information is available online from Wiley InterScience or from the author.

Received: October 21, 2009
Published online: February 24, 2010

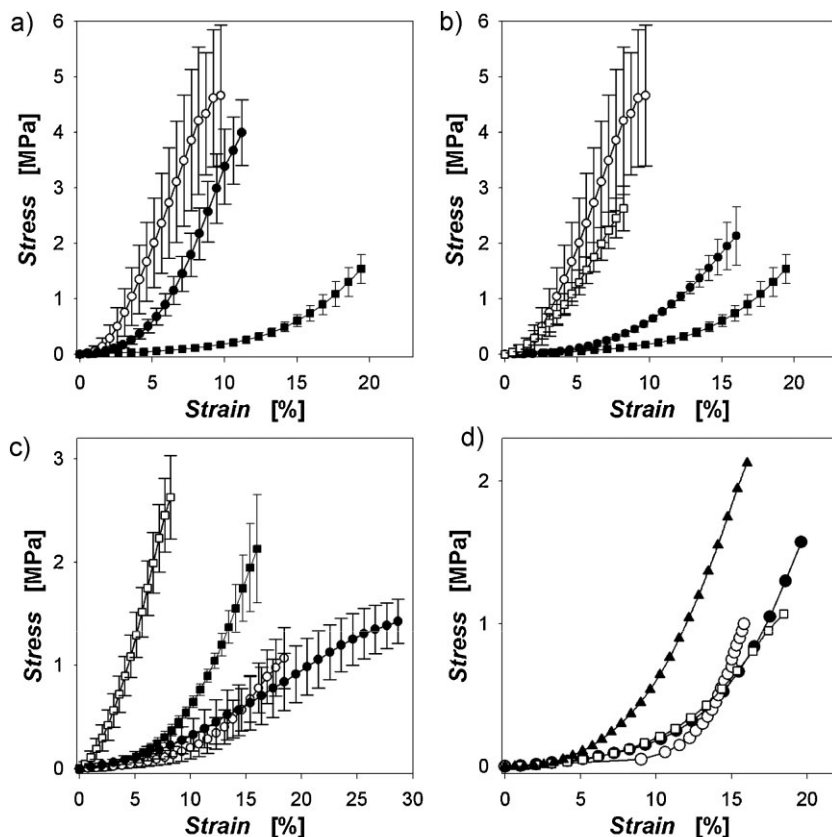


Figure 3. Stress-strain behavior of collagen fiber-reinforced uni- and multilamellar elastin composites. a) Unilamellar sheets reinforced with straight collagen microfibers (○) or microfibers crimped at pre-extension strains of 15% (●) or 30% (■). b) Responses of uni- (○) and multilamellar (□) composites reinforced with straight collagen microfibers are compared to those of unilamellar (■) and multilamellar (●) composites reinforced with fibers crimped at a pre-extension strain of 30%. c) Effect of collagen fiber orientation and crimp. The responses of multilamellar elastin composites reinforced with straight collagen fibers oriented at 0° (□) or ±25° (○) are compared to those multilamellar sheets embedded with collagen fibers crimped at a pre-extension strain of 30% and oriented at 0° (■) or ±25° (●). Data presented as mean ±SD from 3 to 9 samples. d) Uni- (●) and multilamellar (▲) elastin composites reinforced with collagen microfibers crimped at a pre-extension strain of 30% and multilamellar (□) elastin composites embedded with straight fibers oriented at ±25° mimic the mechanical response of glutaraldehyde crosslinked bovine pericardium (○) reported by Sun and colleagues [24].

[1] R. E. Sallach, W. Cui, J. Wen, A. Martinez, V. P. Conticello, E. L. Chaikof, *Biomaterials* **2009**, *30*, 409.
 [2] I. Vesely, *J. Biomech. Eng.* **1998**, *31*, 115.
 [3] J. Gosline, M. Lillie, E. Carrington, P. Guerette, C. Ortlepp, K. Savage, *Philos. Trans. R. Soc. London Ser. B* **2002**, *357*, 121.
 [4] B. Rigby, N. Hirai, J. Spikes, H. Eyring, *J. Gen. Physiol.* **1959**, *43*, 265.

[5] J. Diamant, A. Keller, E. Baer, M. Litt, R. G. Arridge, *Proc. R. Soc. London Ser. B* **1972**, *180*, 293.
 [6] A. Hiltner, J. Cassidy, E. Baer, *Annu. Rev. Mater. Sci.* **1985**, *15*, 455.
 [7] L. J. Gathercole, A. Keller, *Matrix* **1991**, *11*, 214.
 [8] P. B. Canham, P. Whittaker, S. E. Barwick, M. E. Schwab, *Can. J. Physiol. Pharmacol.* **1992**, *70*, 296.
 [9] B. de Campos Vidal, *Micron* **2003**, *34*, 423.
 [10] A. D. Freed, T. C. Doebling, *J. Biomech. Eng.* **2005**, *127*, 587.
 [11] N. D. Broom, *Connect. Tissue Res.* **1978**, *6*, 37.
 [12] S. L. Hilbert, L. C. Sword, K. F. Batchelder, M. K. Barrick, V. J. Ferrans, *J. Biomed. Mater. Res.* **1996**, *31*, 503.
 [13] N. Bowden, S. Brittain, A. Evans, J. Hutchinson, G. Whitesides, *Nature* **1998**, *393*, 146.
 [14] A. Volynskii, S. Bazhenov, O. Lebedeva, N. Bakeev, *J. Mater. Sci.* **2000**, *35*, 547.
 [15] C. Harrison, C. Stafford, W. Zhang, A. Karim, *Appl. Phys. Lett.* **2004**, *85*, 4016.
 [16] D. Y. Khang, H. Jiang, Y. Huang, J. A. Rogers, *Science* **2006**, *311*, 208.
 [17] D. H. Kim, J. H. Ahn, W. M. Choi, H. S. Kim, T. H. Kim, J. Song, Y. Y. Huang, Z. Liu, C. Lu, J. A. Rogers, *Science* **2008**, *320*, 507.
 [18] D. Y. Khang, J. Xiao, C. Kocabas, S. MacLaren, T. Banks, H. Jiang, Y. Y. Huang, J. A. Rogers, *Nano Lett.* **2008**, *8*, 124.
 [19] Y. Sun, W. M. Choi, H. Jiang, Y. Y. Huang, J. A. Rogers, *Nat. Nanotechnol.* **2006**, *1*, 201.
 [20] E. Wright, R. McMillan, A. Cooper, R. P. Apkarian, V. P. Conticello, *Adv. Funct. Mater.* **2002**, *12*, 149.
 [21] D. H. Bergel, *J. Physiol.* **1961**, *165*, 445.
 [22] S. E. Dahms, H. J. Piechota, R. Dahiya, T. F. Lue, E. A. Tanagho, *Br. J. Urol.* **1998**, *82*, 411.
 [23] R. Sodian, S. P. Hoerstrup, J. S. Sperling, S. Daebritz, D. P. Martin, A. M. Moran, B. S. Kim, F. J. Schoen, J. P. Vacanti, J. E. Mayer, Jr, *Circulation* **2000**, *102*, III22.
 [24] D. Mohan, J. W. Melvin, *J. Biomech. Eng.* **1982**, *15*, 887.
 [25] W. Sun, M. Sacks, G. Fulchiero, J. Lovekamp, N. Vyavahare, M. Scott, *J. Biomed. Mater. Res. Part A* **2004**, *69*, 658.
 [26] C. A. Pezowicz, P. A. Robertson, N. D. Broom, *J. Anat.* **2005**, *207*, 299.
 [27] P. D. Ballyk, C. Walsh, J. Butany, M. Ojha, *J. Biomech. Eng.* **1998**, *31*, 229.
 [28] H. J. Salacinski, S. Goldner, A. Giudiceandrea, G. Hamilton, A. M. Seifalian, A. Edwards, R. J. Carson, *J. Biomater. Appl.* **2001**, *15*, 241.
 [29] U. Klinge, B. Klosterhalfen, J. Conze, W. Limberg, B. Obolenski, A. P. Ottinger, V. Schumpelick, *Eur. J. Surg.* **1998**, *164*, 951.
 [30] J. M. Caves, V. Kumar, J. Wen, W. Cui, A. Martinez, R. P. Apkarian, J. Coats, K. Berland, E. L. Chaikof, *J. Biomed. Mater. Res. Part B*, in press.